INFLUENCE OF ANODIC ANGLES ON CORROSION CRACK PATTERN IN REINFORCED CONCRETE

Afra Omara[1], Amged O. Abdelatif [2]

[1&2]Department of Civil Engineering, Faculty of Engineering, University of Khartoum,

afra.omara@gmail.com Amged.Abdelatif@uofk.edu

مُسْتَخْلَص

تدهور المنشأت الخرسانية المسلحة الناجمة عن التآكل بفعل الصدأ الناتج من الكلوريد هو أحد المشاكل الرئيسية لديمومة المنشأت الخرسانية المسلحة. أثبتت الأبحاث الحديثة أن موقع وحجم الزوايا الأنودية والكاثودية لها تأثير قوي على نمط تشقق الخرسانة ومعدل الصدأ وأن نسب الزوايا الأنودية الي الكاثودية لها تأثير على الضرر الناجم عن الصدأ. جميع الأبحاث السابقة درست تأثير الزوايا الأنودية المختلفة نظريا ولكن لم يتم رصد اي اختبارات معملية. في هذه الورقة ، سيتم دراسة تأثير الزوايا الأنودية المختلفة على نمط شقوق الصدأ ومعدل الصدأ معمليا من خلال تطبيق اختبار تسريع الصدأ مع زوايا أنودية مختلفة (360 درجة و 180 درجة و 60 درجة) ونسبة فقدان كتلة الحديد المسلح وقوة الترابط بين الحديد و الخرسانة للعينات. تظهر النتائج أن الزوايا الأنودية المختلفة لها تأثير قوي على نمط تشقق الخرسانة ، معدل الصدأ وقوة الترابط. ثبت أيضا أن التقنيات المعملية المبتكرة في هذه الدراسة يمكن استخدامها لأختبار تأثير الزوايا الأنودية المختلفة.

ABSTRACT

Deterioration of reinforced concrete structures caused by chloride-induced corrosion is one of the main problems for durability in reinforced concrete structures. Recent researches demonstrate that position and size of anodic and cathodic angles have strong influence on crack pattern and corrosion rate and the anodic-cathodic ratios have influence on corrosion-induced damage. All previous researches considered studying the influence of different anodic angles numerically but no experimental investigations were found. In this paper, the influence of different anodic angles on corrosion crack pattern and corrosion rate is investigated experimentally by applying accelerated corrosion test using impressed voltage technique to centrally reinforced concrete cylinders with different anodic angles (360°, 180° and 60°). Current-Time relationship, percentage of steel mass loss and bond strength of the corroded samples are discussed. The results show that the different anodic angles have strong influence on the corrosion crack pattern, corrosion rate and bond strength. Also, it is demonstrated that the developed experimental techniques in this study can be used to investigate the influence of different anodic angles.

Keywords: *Corrosion, anode, cathode, accelerated corrosion test, crack pattern, corrosion rate.*

1 Introduction

Corrosion of reinforcing steel is the leading cause of deterioration in reinforced concrete structures [1]. When steel corrodes the resulting rust has two to six times the volume of the original steel [2]. This expansion creates circumferential tensile stresses in concrete, which can eventually cause cracking, spalling of the concrete cover, loss of bond and reduction in member strength [1,2].

In the normal conditions, reinforcing steel in concrete is highly resistant to corrosion because of the highly alkaline environment which provided by good quality concrete [3]. The corrosion reaction can only occur when the passivating layer is destroyed in the presence of oxygen and water [4]. The location of destroyed layer act as anode whiles the rest of intact surface act as chathode.

The corrosion of the reinforced concrete is an electrochemical process. The process involves two chemical reactions at two different locations on the steel surface. To proceed the reactions; an electrical current must flow in a closed loop. The two reactions are known as "anodic" and "cathodic" reactions, and they occur at "anodic" and "cathodic" areas respectively. Figure 1 shows the corrosion Electrochemical process [5].

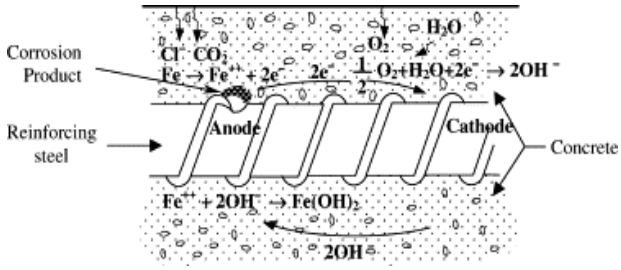

Figure 1: Electrochemical process of corrosion in concrete[6]

2 Effect of corrosion on bond between reinforcing steel and concrete

The corrosion of steel in concrete affects the bond strength in several ways: at early stages the increasing in bar diameter of the corroded reinforcement increases the tensile stresses between the reinforcement and concrete and therefore increasing the friction between the rebar and concrete which is lead to increasing in bond strength [7]. But at later stages of corrosion the tensile stresses causing longitudinal cracking and therefore decreasing the bond strength [7].

Limited literature on the influence of anodic angles on the corrosion crack pattern and corrosion rate were found.

The only literature on the effect of anodic angles on the corrosion crack pattern and corrosion rate were found to be in a recently developed 3D chemo-hygro-thermo mechanical model for steel corrosion in concrete. The model simulating non-mechanical and mechanical processes and their interaction before and after depassivation of steel reinforcement[8].

The 3D chemo-hygro-thermo mechanical model is used to study of the pull-out of the reinforcement bar from the beam-end specimen [9]. The study investigated the influence of anodic angle along the reinforcement bar in the corrosion crack pattern with three different anodic angles (360,180 and 270) as shown in Figure 2.

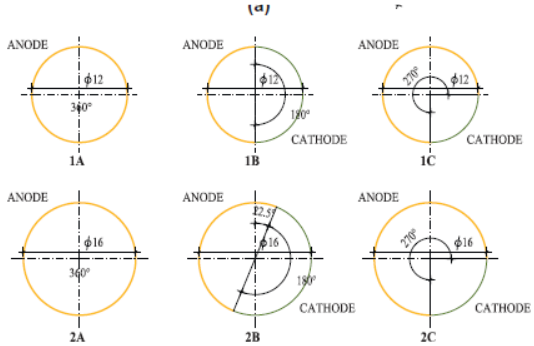

Figure 2: Anodic and Cathodic angles for two groups[9]

The results show that the most realistic crack pattern is obtained for the case where the half of the bar surface (i.e.180°) in comparison with the experimental results.

All previous researches considered comparing the numerical analysis from the model with the experimental results from samples only over the entire circumference (i.e. anodic angle of 360°). Experimental studies were not reported on the investigation of the influence of different anodic angles on the corrosion crack pattern and corrosion rate. Therefore; the aim of this paper is to investigate experimentally the influence of different anodic angles on the corrosion crack pattern, corrosion rate and bond strength.

3 Experimental work

The study was designed to test corrosion parameters of normal reinforced concrete cylinders with different anodic angles (360°, 180° and 60°) under accelerated processes. Two groups of cylinders with different dimension and different concrete covers were used in this research and the accelerated corrosion test was applied to the two groups. Pull out test was applied to the corroded samples (one sample of each sub-group) to determined the bond strength and compare it with the bond strength obtained from the un-corroded samples for each sub-group.

All samples of the present experimental investigation are made of concrete grade 25 N/mm^2 with natural coarse and fine aggregates, w/c ratio equal 0.54 and ordinary portland cement. The steel bar reinforcement used was 16 mm diameter. The concrete was mixed using tap water with 5% of NaCl (of cement content).

3.1 Sample preparation:

Two groups of samples were prepared (Table 1). In the first group two concrete cylinders with size of 150 mm diameter and 300 mm height (G 150-360) were casted with a centrally embedded steel reinforcement of size 16

mm diameter. The surface area of the rebar was un-coated (i.e. 360o anodic angle).

In the second group, seven concrete cylinders using four inches pvc pipes with diameter of 100 mm and 200 mm height were casted with a centrally embedded 16 mm diameter steel reinforcement bar. The cylinders were prepared into three sub-groups.

The first sub-group was free of anti-corrosion coating to give an anodic angle of 360° (G 100-360), the second and third sub-groups were coated to give an anodic angle of 180° (G 100-180) and 60° (G 100-60) respectively as shown in Figure 3. The steel reinforcement of all cylinders was provided at a cover of depth 35 m from bottom.

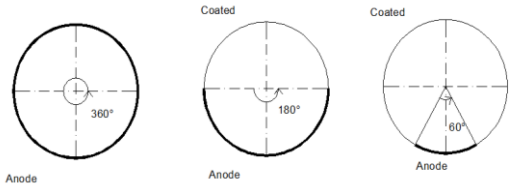

Figure 3: Anodic angles along the cross-section of the reinforcement bar

To prevent entry of oxygen to rebar-concrete junction, a protective layer was used to insure that the cracking occur at the concrete [10].

3.2 Accelerated Corrosion Test

In the present study, the accelerated corrosion test using impressed voltage technique was used. A potential of 12 V (DC power supply) was applied across the tested cylinders [11].The reinforcement steel bar of the concrete cylinders was connected to the positive terminal and stainless steel mesh was connected to the negative terminal of the DC power supply. In this research, steel mesh was used to insure an equally sides flow of current. Both cylinder and stainless steel mesh were partially immersed in 5% NaCl solution for first group samples and the dosage increased to 10% for the second group samples. Figure 4 shows the accelerated corrosion test setup.

Figure 4: Accelerated corrosion test setup

4 Result and discussion

4.1 Current-Time relationship:

The current and the corresponding time (from the beginning of the test (in hours)) are recorded two to three times a day.

Current-time relationships for all reinforced concrete samples of all groups are shown in Figure 5.

Table 1: Two groups Samples properties

Group	Groups ID	Anodic angles	No. of tested sample-s in ACT	Cylinders Dimensions					f_{cu} (N/mm^2)
				Diameter (mm)	Height (mm)	Cover (mm)	Cover from bottom (mm)	Central steel rebar Dia (mm)	
Group (1)	G 150-360	360°	1	150	300	67	35	16	32
Group (2)	G 100-360	360°	3	100	200	42	35	16	35
	G 100-180	180°	1						37
	G 100-60	60°	1						37

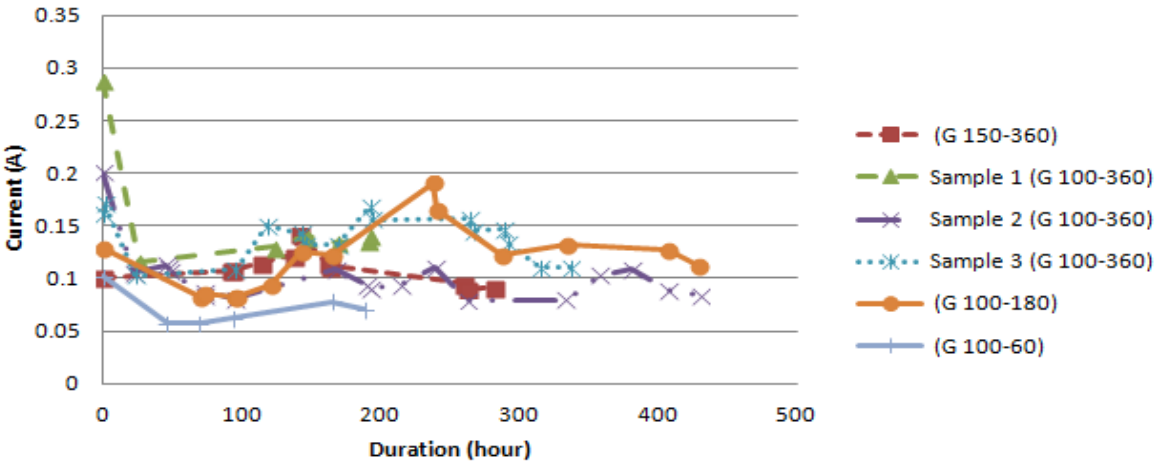

Figure 5: Current-Time relationship for all samples

Decreasing in current is noticed in sample (G 150-360). The cathode at this test setup has to be a stainless steel mesh or plates to insure that the rust will formed at the anode and therefore causing the cracking of concrete [11]. The increasing in current is corresponding to growth of crack and therefore decreasing in electrical resistance [11].

4.2 Crack Pattern:

Crack pattern for the second sample of G 150-360 is shown in Figure 6. The crack starts from the upper part of cylinder down to the lower part.

Figure 6: G 150-360 sample Crack pattern

The first and second sample of group G 100-360 the corrosion happened at the upper part of rebar As a result of that, no increase in current is noticed. The crack patterns for the two samples are shown in Figure 7 and 8 respectively. Also the crack stars from the upper part of cylinder down to the lower part.

Figure 7: G 100-360 sample 1 Crack pattern

Figure 8: G 100-360 sample 2 Crack pattern

It can be noticed from this group that the time of crack initiation in less than the time of crack initiation in G 150-360. This means that the concrete cover have strong influence on the time of crack initiation. The crack pattern for this sample is shown in Figure 9.

Figure 9: G 100-360 sample 3 Crack pattern

The crack pattern for sample 1 of (G 100-180) starts from the top of cylinder at the un-coated side of rebar. And the crack continues in aligned direction down to the lower part of cylinder near to the coated side of rebar as shown in Figure 10.

Figure 10: Crack pattern of G 100-180 sample

The crack pattern for sample 1 (G 100-60) is also starts at the upper part of cylinder near the un-coated side of rebar and continues perpendicularly to the lower part of cylinder as shown in Figure 11.

4.3 Corrosion rate measurements and results:

The percentage of mass loss of corroded reinforcement (C_t) can be calculated using Equation (1) below[10].

$$C_t = \frac{m}{m_i} \times 100 \qquad (1)$$

Where:

m_i = mass of original metal, m = mass loss (in grams) of corroded reinforcement and can be determined by applying Faraday's law as shown in equation (2) below [10]:

$$m = \frac{Q w_a}{nF} \qquad (2)$$

Where:

Q = the total charge passed and can be calculated by getting the area under the curve of current-time relationship, w_a = atomic molar mass (w_a= 55.847 g/mol for Fe), n = number of electrons transferred per iron atom =2 and F = 96,487 C/mol.

Therefore, Corrosion rate for all groups can be determined by applying Faraday's law as shown in equation below [10]:

$$r = \frac{i\, w_a}{n\rho F} \qquad (3)$$

Where:

r = corrosion rate (mm/yr), i = corrosion current density which is the ratio of average current to the original area corroding (A/cm^2), ρ = density of steel, w_a , n and F as mentioned above.

Average current passed into the bars (I) can be obtained by dividing the amount of charge (Q) by the total time duration (T) of test.

Corrosion rate (r) and percentage of mass loss (C_t) have been calculated for all groups of cylinders and the results are illustrated in Table 2. More details and calculation are provided elsewhere [12]

Figure 12 shows the percentage of mass loss (%) for all samples. It can be obvious from this figure that the higher percentage of mass loss obtained from sample with anodic angle of 360° and small concrete cover. No significant difference from the higher value was noticed for the sample with anodic angle of 180°.

Figure 11: Crack pattern of G 100-60 sample

Table 2: corrosion rate and percentage of mass loss results for all groups

Group	Sample No.	Current density (A/cm^2)	Mass loss (m) (in gm)	C_t (%)	r (mm/yr)
G 150-360	_	0.00024	9.41	2.27	$8.87*10^{-9}$
G 100-360	1	0.0019	31.55	12.26	$7.02*10^{-8}$
	2	0.000779	28.9	11.245	$2.87*10^{-8}$
	3	0.001497	43.43	16.8	$5.52*10^{-8}$
G 100-180	_	0.002232	41.34	16.06	$8.23*10^{-8}$
G 100-60	_	0.000549	1.485	0.58	$2.02*10^{-8}$

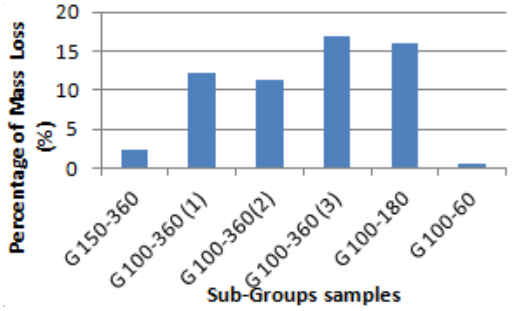

Figure 12: Percentage of Mass Loss (%) for all samples

4.4 Pull out Test Measurement and Results

Load-slip relationship for all samples of G 150-360, G 100-360 and G 100-60 are shown in Figure 13. No records for the corroded sample of G 100-180 because it failed before applying the pull out test. All cylinders loaded up to failure (pulled-out).

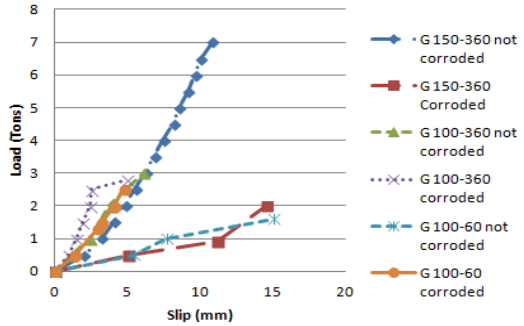

Figure 13: Load-slip relationship for all samples

The corroded rebar and failed cylinders of all tested samples of G 150-360, G 100-360, G 100-180 and G 100-60 are shown in Figures 14, 15, 16 and 17 respectively.

Figure 14: corroded rebar and cylinder of G 150-360

Figure 15: Corroded rebar and cylinder of G 100-360 sample 3

Figure 16: Corroded rebar and cylinder of G 100-180

Figure 17: corroded rebar and cylinder of G 100-60 sample

4.4 Bond strength of corroded samples:

The ultimate bond strength for all tested samples was calculated by the equation 4 below:

$$\sigma_b = \frac{P_b}{\pi D(\frac{anodic\ angle}{360°})l} \quad (4)$$

Where:

σ_b = the ultimate Bond strength (N/mm^2)

P_b = bond failure load (N)

D = bar diameter (mm)

l = embedded length (mm)

The results of bond strength calculation for all tested samples were illustrated in Figure 18.

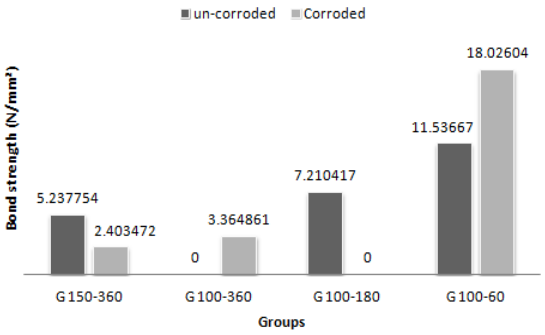

Figure 18: Bond Strength for all tested samples

From the above chart it can be noticed that bond strength increases with the decreasing in anodic angles (whether for corroded or un-corroded samples). For the samples of G 150-360 the bonding strength for the un-corroded sample is higher than the corroded sample. But for G 100-60 the accelerated corrosion test duration was less than the other samples, therefore the bonding strength for the un-corroded sample is less than the corroded sample. This means that the corrosion decreases the bond strength for later stages of corrosion and increases to bond strength for early stages of corrosion. This was discussed previously in the introduction [7].

5 Conclusion

Based on the results of this study the following conclusion can be drawn:

- The anodic angles have strong influence on the concrete crack pattern, corrosion rate and Bond strength experimentally.
- The higher percentage of mass loss (%) obtained from the sample with full anodic angle and small concrete cover.
- The study confirms that corrosion increases the bond strength at early stages of corrosion and decreases the bond strength at later stages of corrosion.
- The developed accelerated experiments can be used to investigate the influence of different anodic angles on corrosion crack pattern and corrosion rate.

References

[1] N. Palumbo, “Accelerated Corrosion Testing of Steel Reinforcement in Concrete,” McGill University, 1991.

[2] V. Kumar, R. Singh, and M. A. Quraishi, “A Study on Corrosion of Reinforcement in Concrete and Effect of Inhibitor on Service Life of RCC,” *J. Mater. Enviromental Sci.*, vol. 4, no. 5, pp. 726–731, 2013.

[3] Z. P. Bazant, “Physical Model for Steel Corrosion in Concrete Sea Structures --Theory,” *J. Struct. Div.*, vol. 105, 1979.

[4] C. M. Hansson, A. Poursaee, and S. J. Jaffer,

"Corrosion of reinforcing bars in concrete," *The Masterbuilder*, 2012.

[5] A. Bentur, N. Berke, and S. Diamond, *Steel corrosion in concrete: fundamentals and civil engineering practice*. CRC Press, 1997.

[6] S. Ahmad, "Reinforcement corrosion in concrete structures, its monitoring and service life prediction—a review," *Cem. Concr. Compos.*, vol. 25, no. 4–5, pp. 459–471, May 2003.

[7] FI du Béton - Bulletin, *Bond of reinforcement in concrete: state-of-art report*. 2000.

[8] J. Ožbolt, F. Oršanić, and G. Balabanić, "Modelling processes related to corrosion of reinforcement in concrete: coupled 3D finite element model," *Struct. Infrastruct. Eng.*, vol. 13, no. 1, pp. 135–146, 2017.

[9] J. Ožbolt, F. Oršanić, and G. Balabanić, "Modeling pull-out resistance of corroded reinforcement in concrete: Coupled three-dimensional finite element model," *Cem. Concr. Compos.*, vol. 46, pp. 41–55, 2014.

[10] E. K. Benito, M. S. Madlangbayan, N. M. S. Tabucal, M. B. Sundo, and P. Perlie, "Corrosion Damage Measurement on Reinforced Concrete by Impressed Voltage Technique and Gravimetric Method," *Int. J. GEOMATE*, vol. 13, no. 39, pp. 198–205, 2017.

[11] S. Deb, "Accelerated Short-Term Techniques to Evaluate Corrosion in Reinforced," *The Masterbuilder*, 2012.

[12] A. Omara and A. Abdelatif, "Influence of Anodic Angles on Corrosion Crack Pattern in Reinforced Concrete," University of Khartoum, 2018.